Original Article

Value of carotid intima thickness in assessing advanced carotid plaque vulnerability: a study based on carotid artery ultrasonography and carotid plaque histology

Ya-Chao Zhao[1], Jia Zhang[1], Fei Wang[2], Yi-Ming He[2], Ming-Jun Xu[1], Dong-Hai Wang[2], Mei Zhang[1]

[1]National Key Laboratory for Innovation and Transformation of Luobing Theory, The Key Laboratory of Cardiovascular Remodeling and Function Research, Chinese Ministry of Education, Chinese National Health Commission and Chinese Academy of Medical Sciences, Department of Cardiology, Qilu Hospital of Shandong University, Jinan, China; [2]Neurosurgery Department, Qilu Hospital of Shandong University, Jinan, China

Contributions: (I) Conception and design: MJ Xu, DH Wang, M Zhang; (II) Administrative support: DH Wang, M Zhang; (III) Provision of study materials or patients: All authors; (IV) Collection and assembly of data: YC Zhao, J Zhang, F Wang, YM He; (V) Data analysis and interpretation: YC Zhao, MJ Xu; (VI) Manuscript writing: All authors; (VII) Final approval of manuscript: All authors.

Correspondence to: Mei Zhang, MD, PhD, FACC. National Key Laboratory for Innovation and Transformation of Luobing Theory, The Key Laboratory of Cardiovascular Remodeling and Function Research, Chinese Ministry of Education, Chinese National Health Commission and Chinese Academy of Medical Sciences, Department of Cardiology, Qilu Hospital of Shandong University, No. 107 Wenhuaxi Road, Jinan 250012, China. Email: daixh@vip.sina.com; Dong-Hai Wang, MD. Neurosurgery Department, Qilu Hospital of Shandong University, No. 107 Wenhuaxi Road, Jinan 250012, China. Email: drwangdonghai@163.com; Ming-Jun Xu, MD, PhD. National Key Laboratory for Innovation and Transformation of Luobing Theory, The Key Laboratory of Cardiovascular Remodeling and Function Research, Chinese Ministry of Education, Chinese National Health Commission and Chinese Academy of Medical Sciences, Department of Cardiology, Qilu Hospital of Shandong University, No. 107 Wenhuaxi Road, Jinan 250012, China. Email: xmj223@163.com.

Background: Research has shown that carotid intima-media thickness (CIMT) could help to predict carotid plaque (CP) progression in patients with mild carotid stenosis. However, the debate continues as to the value of carotid intima thickness (CIT) in monitoring the development of CP in patients with severe carotid stenosis. This study sought to evaluate the relationships between CIT and the ultrasonic characteristics of CP and to analyze the value of CIT and the ultrasonic parameters of CP in assessing plaque vulnerability in advanced human carotid atherosclerosis.

Methods: A total of 55 individuals who underwent carotid endarterectomy (CEA) were included in the study (mean age: 65±7 years; female: 9.1%). CIMT and CIT were examined at the common carotid artery (CCA). Plaque textural features, such as the gray-scale median (GSM), superb microvascular imaging (SMI) level, and total plaque area (TPA), were also identified. A Spearman correlation coefficient analysis was performed to examine the relationship between CIT and the ultrasonic parameters of CP. The CIT of various plaque types was compared. Receiver operating characteristic (ROC) curves were used to analyze the diagnostic values of the ultrasound characteristics to evaluate CP vulnerability.

Results: The mean CIT of all the participants was 0.382±0.095 mm, the mean CIT of the participants with stable plaques was 0.328±0.031 mm, and the mean CIT of participants with vulnerable plaques was 0.424±0.106 mm (P<0.001). CIT was associated with the SMI level (Spearman's correlation coefficient: r=0.392, P=0.005), TPA (Spearman's correlation coefficient: r=0.337, P=0.012). Patients with thicker CIT had larger lipid cores, higher levels of plaque vulnerability, and more intraplaque hemorrhages (IPHs). The areas under the ROCs (AUCs) with 95% confidence interval (CI) for CIMT, CIT, the SMI level, the GSM, the TPA, and the combined model for identifying vulnerable plaques were 0.673 (0.533–0.793), 0.849 (0.727–0.932), 0.771 (0.629–0.879), 0.669 (0.529–0.790), 0.858 (0.738–0.938), and 0.949 (0.854–0.990), respectively.

Conclusions: CIT was associated with both the histology and ultrasonic features of CP. CIT may be helpful in the detection of severe CP development.

Keywords: Carotid intima thickness (CIT); superb microvascular imaging (SMI); gray-scale median (GSM); total plaque area (TPA); plaque vulnerability

Submitted Aug 22, 2023. Accepted for publication Dec 20, 2023. Published online Jan 23, 2024.
doi: 10.21037/qims-23-1193
View this article at: https://dx.doi.org/10.21037/qims-23-1193

Introduction

The primary causes of death worldwide are cardiovascular (CV) disorders, particularly coronary artery disease (CAD) and stroke, and 75% of CAD deaths occur in low- and middle-income nations (1,2). The key factor causing CV disorders is atherosclerosis, which mostly affects the aorta, carotid artery, and other large and medium-sized arteries (3,4). CV events are more likely to occur in vulnerable plaques, which are distinguished by a thin fibrous cap, a bigger lipid core, less collagen, ulceration, non-calcification, intraplaque hemorrhage (IPH), and the infiltration of inflammatory cells (5,6). Therefore, the most crucial factors in the prevention of CAD and stroke are the early diagnosis of vulnerable plaques and timely treatment.

Using ultrasound to assess carotid plaque (CP) progression, studies have shown that the gray-scale median (GSM) of CP was related to the type and vulnerability of the plaque (7,8). The total plaque area (TPA) is another precise, non-invasive approach for detecting subclinical atherosclerosis, and is a better indicator of CV risk than intima-media thickness (IMT) (9-11). One of the factors contributing to the progression of atherosclerotic lesions and the subsequent consequences, including IPH and plaque rupture, is intraplaque neovascularization (IPN) (12,13). Superb microvascular imaging (SMI) is a novel ultrasound technology that provides vascular information by extracting flow signals from large vessels or smaller microvasculature through advanced filtering algorithms and suppressing background tissue movement without suppressing any slow flow signals (14-16), and may be a promising method for diagnosing IPN (13).

Numerous experimental and cross-sectional investigations have shown that increased carotid intima-media thickness (CIMT) is a promising early marker and a reliable indicator of early atherosclerosis (17,18). However, CIMT does not appear to provide any significant benefit in monitoring the development of CP in patients with severe carotid artery stenosis (19). According to recent research, CIMT is more likely to reflect adaptive changes in response to increased shear stress with aging and is less likely to reflect atherosclerotic alterations (20). As an alternative, carotid intima thickness (CIT) might be measured to monitor the development of carotid stenosis. It is well known that the development of subintimal lipid deposits and the beginning of inflammation are two characteristics of atherosclerosis (21,22). Lipid deposits form in the subintima of arteries throughout the body during the progression of atherosclerosis. Recent studies have also revealed a relationship between the classic atherosclerotic risk factors and CIT, which has good diagnostic value for ischemic stroke and CAD and is helpful in identifying subtypes of ischemic stroke (23,24). Therefore, employing CIT to track the advancement of CP could have great clinical value.

The current study not only sought to determine whether CIT was related to the ultrasonic characteristics of CP but also sought to examine the correlations among the CP ultrasonic characteristics, CIT, and the histological features of vulnerable plaque. Specifically, this study sought to identify any potential associations between the common carotid artery (CCA) indicators CIT and CP that might be used to evaluate vulnerable CP. We present this article in accordance with the STARD reporting checklist (available at https://qims.amegroups.com/article/view/10.21037/qims-23-1193/rc).

Methods

Study population

In this prospective study, we consecutively enrolled 60 adult patients referred for carotid endarterectomy (CEA) at a single center from October 2021 to November 2022. Patients who were eligible for CEA were included in the study. To determine the severity of the carotid stenosis, all patients underwent digital subtraction angiography (DSA). To be eligible for inclusion in this study, the patients have had carotid stenosis >50% according to the North American Symptomatic Carotid Endarterectomy Trial (NASCET) criteria accompanied by symptoms (transient ischemic attack, stroke, or amaurosis fugax), or carotid stenosis >70% without evident symptoms. Patients who did not have atherosclerotic carotid disease or who did not qualify for

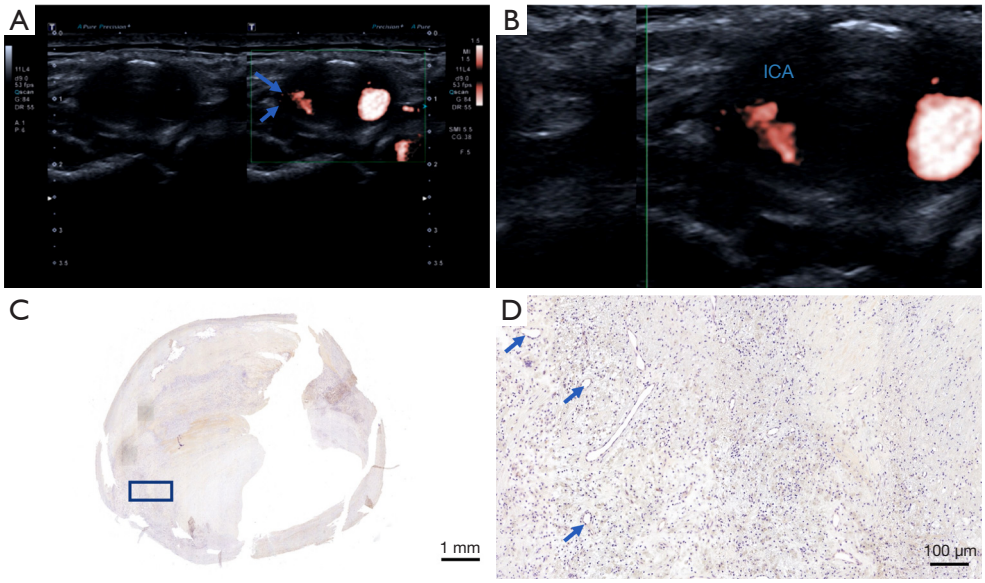

Figure 1 SMI measurement and its relationship to histopathology. (A) Plaque SMI examination. A cross-section of the entire patch was displayed, with the B mode on the left and the SMI on the right. The light color denotes a positive signal (blue arrows). (B) A magnification of the SMI image in (A) provides a more accurate depiction of a positive SMI signal. (C) Histological slice of the plaque (CD34 staining, ×1). (D) A magnification of the patch's shoulder (which is depicted by the blue box in C), several CD34 positive neovessels are present (arrows, ×10). ICA, internal carotid artery; SMI, superb microvascular imaging.

CEA were excluded from the study. Next, all the eligible participants underwent CEA, and CPs were removed to preserve the plaque structure. The study was conducted in accordance with the Declaration of Helsinki (as revised in 2013). The study was approved by the Ethics Committee of Shandong University Qilu Hospital (No. KYLL-2020-183) and informed consent was obtained from all the patients.

Gender, age, body mass index (BMI), blood pressure, total cholesterol, triglycerides, low-density lipoprotein cholesterol, high-density lipoprotein cholesterol, and fasting blood glucose (GLU) data were obtained. Additionally, information about smoking, diabetes mellitus (DM), smoking history, and medications like statins, antiplatelet medications, and antihypertensive medications were simultaneously recorded. Hypertension was defined as systolic blood pressure (SBP) ≥140 mmHg and/or diastolic blood pressure (DBP) ≥90 mmHg, or taking antihypertensive drugs (25). DM refers to fasting blood GLU ≥7.0 mmol/L and/or blood GLU ≥11.1 mmol/L two hours postprandially, or taking hypoglycemic drugs (26).

B-mode ultrasonography of CP

An ultrasound machine (AplioI900, Canon-Toshiba Ultrasonic, Toshiba-Ken, Japan) with a 4–11 MHz high-frequency linear transducer (PLT-704SBT) was used to perform the carotid ultrasonography. Plaques in the longitudinal section of the carotid artery were scanned, and the image with the largest plaque area was captured and used for further research. Software incorporated inside the machine was used to compute plaque area. TPA was defined as the sum of all plaque regions visible in the longitudinal images (9). The gray level of the entire plaque was represented by the GSM. For the image normalization and gray pixel analysis of the GSM, Adobe Photoshop 6.0 (Adobe Systems, Inc., San Jose, CA, USA) was used. The outside membrane was set to 190 and the blood to 0 (the gray-scale range was 0 to 255; black =0 and white =255) (27,28). TPA and GSM were measured three times and averaged.

SMI ultrasonography and image analysis

The ultrasound scanner's settings were changed to the SMI mode to present a dual image of the plaque side by side in B mode, and color SMI after the plaque's echogenicity was evaluated in B mode (*Figure 1A*). The region of interest of the SMI was applied to the entire plaque. The other SMI settings were as follows: mechanical index, 1.5; frame rate, 50–60 fps,

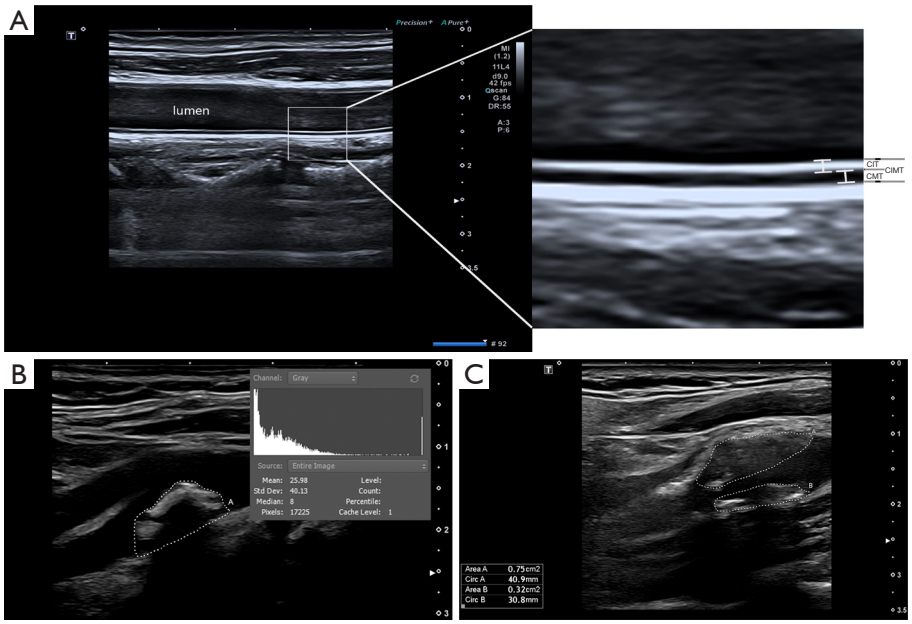

Figure 2 Measurements of CIT, GSM, and TPA. (A) Measurements of the CIT, CMT, and CIMT. Longitudinal-axis image of the carotid artery 3 cm before the carotid bifurcation on the left, and a zoom image of the region of interest on the right. (B) Carotid plaque with a histogram of gray-tone frequency distribution of pixels in the normalized image's selected area (plaque). (C) Carotid plaque area measurement. Each plaque was measured in a longitudinal perspective in the plane where the plaque is maximal, and a cursor was traced around the perimeter of the cross-section. The microprocessor in the duplex scanner displays the plaque's cross-sectional area (cm^2). CIT, carotid intima thickness; CMT, carotid media thickness; GSM, gray-scale median; TPA, total plaque area; CIMT, carotid intima-media thickness.

SMI velocity, 0.8–1.5 cm/s; and dynamic range, 55–60 dB. The plaques were first observed on the longitudinal section and then on the cross-section for 30 seconds. Dynamic enhancement signals or intraplaque microvascular flow (IMVF) signals were captured after the static enhancement signal was eliminated (*Figure 1B*). The IMVF signals were classified as follows: grade 0, no IMVF signals in the plaque or IMVF signals confined to the adjacent adventitia; grade 1, moving IMVF signals confined to the adventitial side; grade 2, moving IMVF signals at the plaque shoulder; grade 3, IMVF signals moving to the plaque core; and grade 4, extensive IMVF signals (29). Next, an immunohistochemical analysis of the endothelial cells was performed with CD34 (*Figures 1C,1D*). Finally, the histology and SMI correlation of the specimens were examined.

CIT, CIMT ultrasonography, and image analysis

The scanning was performed longitudinally from the proximal end of the CCA to the bifurcation of the CCA to ensure that the entire 3 cm section of the CCA proximal to the bifurcation was fully scanned. At a depth of no more than 3–4 cm, the focus was adjusted to provide the best near and far wall resolution. The gain settings were tuned with the goal of generating a clear separation between the intima and media layers. In the long axis view during systole, CIT and CIMT were assessed on the plaque-free distal wall of the bilateral CCAs at 1.5, 2, and 2.5 cm prior to carotid bifurcation (*Figure 2*). CIT was defined as the distance from the leading edge of the lumen-intima interface to the intima-media interface of the far wall, and CIMT was defined as the distance from the leading edge of the lumen-intima interface to the leading edge of the media-adventitia interface of the far wall. Previous research has shown that this method of measuring CIT and CIMT is accurate (30,31). Using built-in software, an offline analysis of the CCA pictures taken during systole was performed. The final CIT was determined by averaging the bilateral CIT measurements of each subject.

Tissue processing and histological analysis

The CEA specimens were fixed in 4% formaldehyde and cut into 2- to 3-mm transverse sections. Following

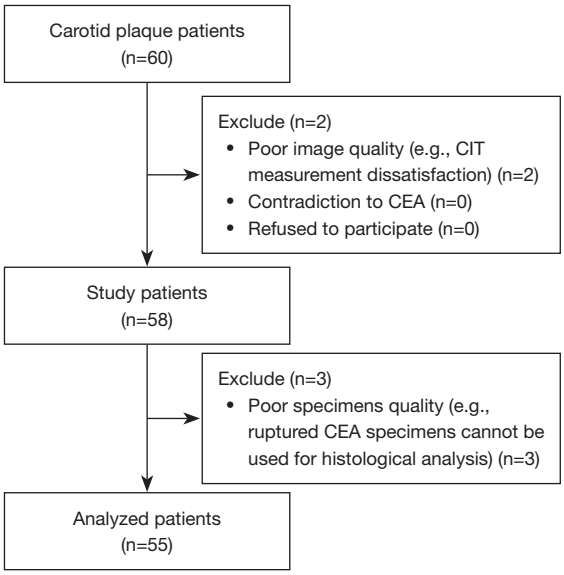

Figure 3 Flowchart of the patient recruitment process. CIT, carotid intima thickness; CEA, carotid endarterectomy.

dehydration and paraffin embedding, the plaques were sectioned at 5 μm in a longitudinal plane. Hematoxylin and eosin was used to stain each segment, while Sirius Red was used to detect collagen. The following markers were used to stain all sections: CD3 (Abcam Cat# ab16669, RRID:AB_443425, Cambridge, UK) for lymphocytes, CD34 (Abcam Cat# ab81289, RRID:AB_1640331) for endothelial cells, CD68 (Abcam Cat# ab125212, RRID:AB_10975465) for macrophages, and α-SMA (Abcam Cat# ab5694, RRID:AB_2223021) for smooth muscle cells. Based on their characteristics, the plaques were defined as follows: definitely stable (predominantly fibrous, few inflammatory cells, and an intact cap); probably stable (one feature of instability, such as a small hemorrhage, or the infiltration of inflammatory cells); probably unstable (inflammation, a thin cap, and a large core but no rupture); or definitely unstable (a rupture, thrombus, a large hemorrhage, and a thin inflamed cap). Lovett's classification and the American Heart Association (AHA) coronary plaque classification system were used to categorize all the plaque features (32).

Statistical analysis

SPSS25.0 (SPSS Inc., Chicago, IL, USA) was used for the statistical analysis. The continuous data are presented as the mean ± standard deviation. The categorical data are expressed as the number (percentage). The normality of distribution of the continuous variables was assessed by both measures of skewness and kurtosis and by the Shapiro-Wilk normality test. A two-tailed Student's *t*-test was used to compare continuous variables that follow a normal distribution, and a Mann-Whitney *U* test was used to evaluate non-normal continuous variables. The χ^2 test was developed to compare the categorical variables. A non-parametric Spearman correlation analysis was used to conduct the correlation analysis. Binary logistic regression was used to investigate the diagnostic utility of ultrasonic parameters for plaque vulnerability. Variables with significant contributions in the binary logistics regression analysis were included in the combined models, and the receiver operating characteristic (ROC) curves were plotted. The differences between the ROC curves were assessed using the DeLong test. A two-tailed P<0.05 indicated statistical significance.

Results

Clinical characteristics

In total, 60 participants underwent CEA, of whom three were disqualified due to poor sample quality and two due to subpar picture quality. The patient recruitment process is presented in *Figure 3*. Ultimately, the CIT data from 55 plaques (49 of which also had SMI data) were examined in the study. Among all the plaques, 24 (43.6%) definitely stable or probably stable plaques were classified as stable plaques, and 31 (56.4%) probably unstable or definitely unstable plaques were classified as vulnerable plaques. The clinical characteristics did not differ statistically between the stable and vulnerable plaques (*Table 1*).

Carotid ultrasound

The CIMT and CIT of patients with vulnerable plaques were thicker than those of patients with stable plaques (0.877±0.087 *vs.* 0.813±0.115 mm, P=0.022 for CIMT, and 0.424±0.106 *vs.* 0.328±0.031 mm, P<0.001 for CIT). In total, 49 plaques were examined for SMI, including 21 stable plaques and 28 vulnerable plaques. Meanwhile, the vulnerable plaques had more SMI signals, larger TPAs, and lower GSM values than the stable plaques (P<0.05 for all) (*Table 2*).

Correlations between CIT and plaque ultrasonic appearance

Figure 4 illustrates the correlations between CIT and

Table 1 Clinical characteristics of patients with stable and vulnerable plaques

Characteristics	All patients (n=55)	Stable plaques (n=24)	Vulnerable plaques (n=31)	P value
Age (years)	65±7	65±7	65±7	0.970
Female	5 (9.1)	1 (4.2)	4 (12.9)	0.373
BMI (kg/m^2)	24.74±3.08	24.84±2.99	24.66±3.19	0.829
Smoking	33 (60.0)	17 (70.8)	16 (51.6)	0.190
Alcohol	28 (50.9)	12 (50.0)	16 (51.6)	0.808
Hypertension	41 (74.5)	19 (79.2)	22 (71.0)	0.489
SBP (mmHg)	140.75±18.64	144.29±19.62	138±17.68	0.218
DBP (mmHg)	76.42±9.48	76.54±9.23	76.32±9.82	0.933
DM	11 (20.0)	6 (25.0)	5 (16.1)	0.634
CAD	22 (40.0)	7 (29.2)	15 (48.4)	0.149
Stroke or TIA	32 (58.2)	12 (50.0)	20 (64.5)	0.279
Antiplatelet	43 (78.2)	17 (70.8)	26 (83.9)	0.246
Statins	37 (67.3)	14 (58.3)	23 (74.2)	0.214
Antihypertensive drugs	41 (74.5)	19 (79.2)	22 (71.0)	0.489
TC (mmol/L)	3.54±0.79	3.65±0.92	3.44±0.67	0.338
TG (mmol/L)	1.37±0.62	1.39±0.66	1.35±0.60	0.821
LDL-C (mmol/L)	1.97±0.56	2.04±0.62	1.90±0.50	0.362
HDL-C (mmol/L)	1.04±0.28	1.04±0.32	1.03±0.25	0.855
GLU (mmol/L)	5.44±1.02	5.66±1.25	5.27±0.78	0.247

Values are shown as the mean ± standard deviation or numbers (%). BMI, body mass index; SBP, systolic blood pressure; DBP, diastolic blood pressure; DM, diabetes mellitus; CAD, coronary artery disease; TIA, transient ischemic attack; TC, total cholesterol; TG, triglycerides; LDL-C, low-density lipoprotein cholesterol; HDL-C, high-density lipoprotein cholesterol; GLU, fasting glucose.

Table 2 Ultrasonic parameters in patients with stable and vulnerable plaques

Parameters	All patients (n=55)	Stable plaques (n=24)	Vulnerable plaques (n=31)	P value
CIMT (mm)	0.849±0.104	0.813±0.115	0.877±0.087	0.022*
CIT (mm)	0.382±0.095	0.328±0.031	0.424±0.106	<0.001*
SMI	31 (63.3)	8 (38.1)	23 (82.1)	0.002*
GSM	33.46±21.20	40.74±25.08	27.83±15.87	0.032*
TPA (mm^2)	77.82±34.31	55.85±20.01	94.83±33.57	<0.001*

Values are shown as mean ± standard deviation or numbers (%). Forty-nine plaques were examined for SMI, including 21 stable plaques and 28 vulnerable plaques. *, the values are statistically significant. CIMT, carotid intima-media thickness; CIT, carotid intima thickness; SMI, superb microvascular imaging; GSM, greyscale median; TPA, total plaque area.

the SMI level (r=0.392, P=0.005), and CIT and the TPA (r=0.337, P=0.012). In the multiple linear regression analysis, none of the parameters assessed reached statistical significance.

Histologically determined plaque types and plaque vulnerability

The histological characteristics of the 55 plaques were graded on simple semiquantitative scales as published by

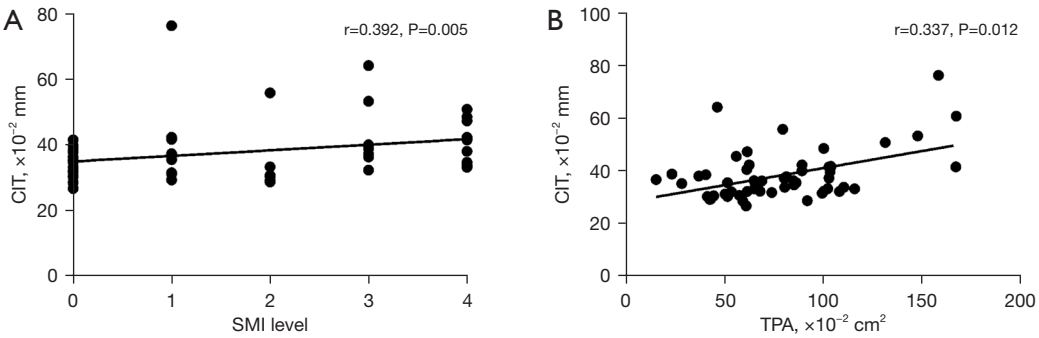

Figure 4 Correlations between CIT and plaque ultrasonic appearance. CIT, carotid intima thickness; SMI, superb microvascular imaging; TPA, total plaque area.

Table 3 Histological characteristics of stable and vulnerable plaques

Characteristics	All patients (n=55)	Stable plaques (n=24)	Vulnerable plaques (n=31)	P value
Lipid core	34 (61.8)	12 (50.0)	22 (71.0)	0.112
Calcification	34 (61.8)	13 (54.2)	21 (67.7)	0.304
Any hemorrhage	24 (43.6)	5 (20.8)	19 (61.3)	0.003*
Any thrombus	6 (10.9)	0	6 (19.4)	0.03*
Thin fibrous cap thickness	21 (38.2)	3 (12.5)	18 (58.1)	0.001*
Fibrous cap rupture	22 (40.0)	6 (25.0)	16 (51.6)	0.046*
Marked fibrous cap infiltration	40 (72.7)	15 (62.5)	25 (80.6)	0.134
Predominantly fibrous	14 (25.5)	10 (41.7)	4 (12.9)	0.015*
Marked foam cells	37 (67.3)	15 (62.5)	22 (71.0)	0.507
Marked inflammatory cells	38 (69.1)	15 (62.5)	23 (74.2)	0.352
Neovascularization	34 (61.8)	11 (45.8)	23 (74.2)	0.032*

Values are shown as numbers (%). *, the values are statistically significant.

Lovett *et al.* (32). Among them, 61.8% had a lipid core (n=34), 61.8% had calcification (n=34), 43.6% had IPH (n=24), and 10.9% had thrombus (n=6). Fibrous cap thickness (FCT) data were available for 49 plaques, 20 of which were stable plaques and 29 of which were vulnerable plaques. Compared with the stable plaques, the vulnerable plaques had thinner FCT, less fibrous tissue, and more IPN, IPH, and thrombus (*Table 3*).

Relationship between plaque types and CIT

The CIT of the patients with plaques with a large lipid core was significantly thicker than that of the patients with plaques with no lipid core (0.44±0.132 *vs.* 0.342±0.052, P=0.021). The CIT of patients with plaques with more infiltrated cells in the fibrous cap was thicker than that of patients with plaques with less infiltrated cells (0.4±0.099 *vs.* 0.3±0.02 mm, P=0.032, for heavy fibrous cap cell infiltration and minor fibrous cap cell infiltration), and the CIT of patients with plaques with IPH was thicker than that of patients with plaques without IPH (0.439±0.079 *vs.* 0.355±0.089 mm, P=0.016, for large IPH and no IPH; 0.411±0.098 *vs.* 0.355±0.089 mm, P=0.028, for small IPH and no IPH). Increased CIT was associated with worse plaque stability (0.431±0.092 *vs.* 0.314±0.006 mm, P=0.013, for definitely unstable and definitely stable; 0.431±0.092 *vs.* 0.331±0.034 mm, P=0.002, for definitely unstable and probably stable; 0.419±0.118 *vs.* 0.331±0.034 mm, P=0.013, for probably unstable and probably stable). The relationships between plaque types and CIT are described in *Figure 5*.

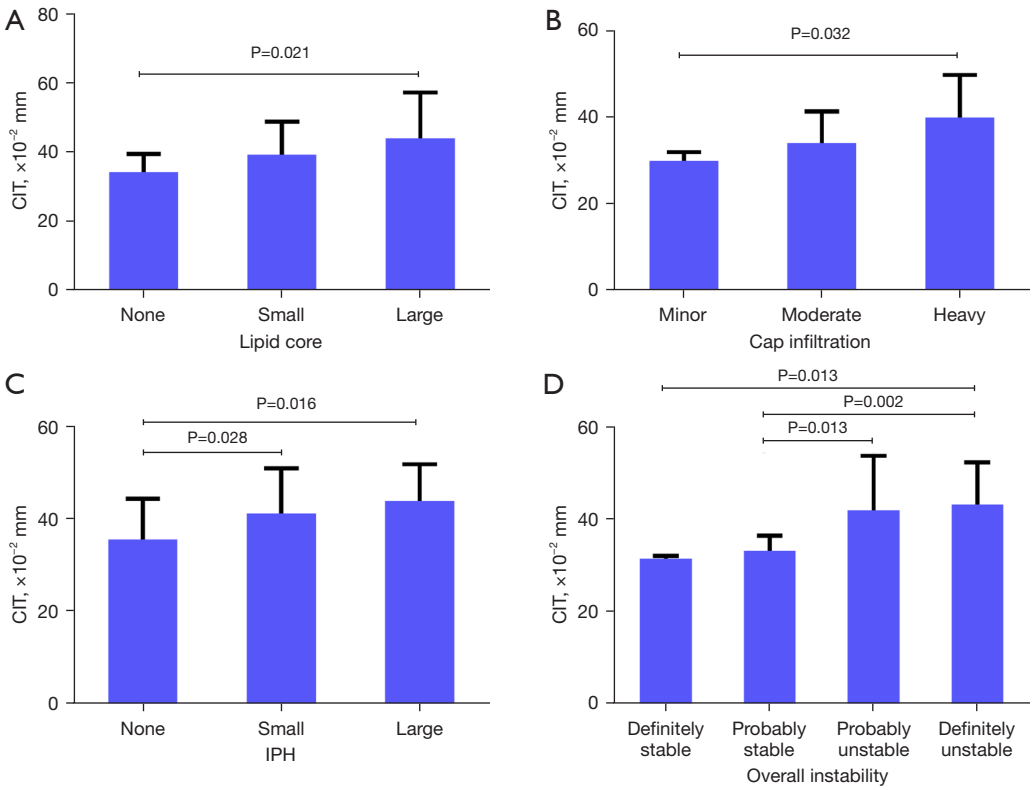

Figure 5 Relations between CIT and plaque types. CIT thickening was associated with larger lipid cores, increased fibrous cap cell infiltration, increased IPH, and worse overall instability. CIT, carotid intima thickness; IPH, intraplaque hemorrhage.

Values of CIMT, CIT, SMI, GSM, and TPA in assessing plaque vulnerability

The areas under the curve (AUCs) with 95% confidence interval (CI) of the CIMT, CIT, SMI, GSM and TPA for predicting plaque vulnerability were 0.673 (0.533–0.793), 0.849 (0.727–0.932), 0.771 (0.629–0.879), 0.669 (0.529–0.790), and 0.858 (0.738–0.938), respectively (*Figure 6*). In relation to the ultrasound parameters for the plaques, the AUC of the TPA was the largest. In relation to the ultrasound parameters for the CCA, the AUC of the CIT was larger than the AUC of the CIMT (0.849 *vs.* 0.673, P=0.026). We also analyzed a combined model of CIT and TPA. The AUC (95% CI) of the combined model was 0.949 (0.854–0.990) with a sensitivity and specificity of 84% and 96%, respectively, when the cut-off value was 0.71, which was significantly larger than the AUCs of the CIMT, CIT, SMI, GSM, and TPA (*Table 4*).

Discussion

In this study, we examined CIT and the ultrasonic and histological manifestation of atherosclerotic plaques in carotid bifurcation. Our results showed that CIT was correlated with the ultrasonic features of CP, including the SMI level and TPA. Additionally, we found that CIT was correlated with the histological characteristics of the plaque, such as the size of the lipid core, the infiltration of the fibrous cap cells, IPH, and overall instability. Further, the CIT had the same importance as the TPA in determining plaque vulnerability and was better able to determine plaque vulnerability than SMI and the GSM.

It is widely recognized that a precise and reliable diagnosis of vulnerable atherosclerotic plaques prior to clinical manifestations is critical for identifying high-risk individuals. Computed tomographic angiography (CTA) is a tool commonly used to examine vulnerable plaques and allows for the precise assessment of the luminal and outer arterial wall dimensions, high-risk plaque burden and morphology, and remodeling patterns (33). Specifically, CTA enables high-risk plaques to be categorized into the following three types: partially calcified, calcified, and non-calcified (including both calcified and non-calcified

plaque tissue) (34). Further, previous studies have shown that CTA can identify plaque development following statin therapy (35). However, due to inadequate imaging resolution, studies have shown that CTA is not very accurate in differentiating between lipids, components of fibrotic tissue, and intraplaque inflammation (36).

High-resolution magnetic resonance imaging (MRI) is currently regarded as the most competitive imaging modality for evaluating the carotid artery wall due to its remarkably high soft-tissue resolution (37). Based on advanced imaging technologies that achieve high spatial resolution, minimal motion interference and black-blood, MRI has shown promise in providing comprehensive details about artery wall morphological parameters, including wall thickness, volume, and plaque burden (38). Moreover, MRI also has a good ability to predict vulnerable plaques with hemodynamic instability (39). However, the presence of flow, motion, or metal susceptibility artifacts, relatively expensive costs, and prolonged examination periods have hindered the widespread adoption of MRI (40). Non-invasive ultrasound is a widely used approach that is rapid, without known radiation, and inexpensive in comparison to other imaging modalities. Additionally, unlike angiography, ultrasonography can display both the lumen and the vessel wall.

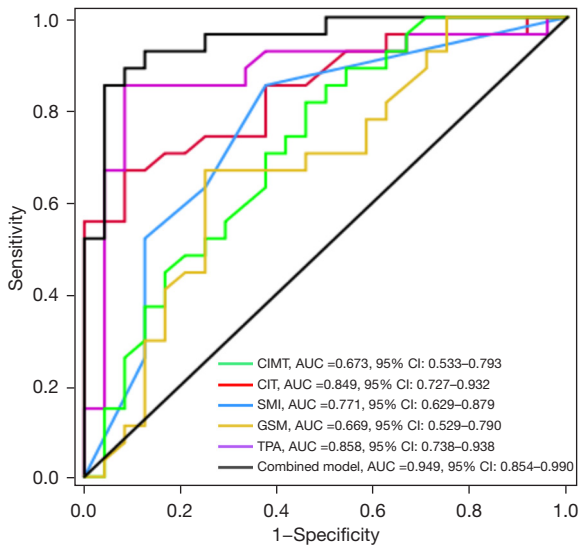

Figure 6 Receiver operating characteristic analysis of different parameters and a combined model for differentiating vulnerable plaques. The combined model, which included the TPA and CIT, had the largest area under the curve. CIMT, carotid intima-media thickness; AUC, area under the receiver operating characteristic curve; CIT, carotid intima thickness; SMI, superb microvascular imaging; GSM, greyscale median; TPA, total plaque area; CI, confidence interval.

Plaque ultrasonography is a critical tool for detecting plaque type and vulnerability (41). Research has shown that plaques with an established histology of high lipid and hemorrhage content had a low GSM (Spearman correlation r=–0.351, P<0.05) and those with a high fibrous content had a high GSM (r=0.411, P<0.001) (42). TPA is also regarded as a reliable indicator for the assessment of vulnerable plaques due to its high repeatability (0.95, 95% CI: 0.83–0.99 for interobserver reliability; 0.96, 95% CI: 0.94–0.97 for intraobserver reliability) (43,44). SMI is a non-invasive technique that can facilitate the visualization of carotid artery IPN and has a sensitivity and specificity of 63% and 100% compared with patients observed Intraplaque enhancement by using contrast-enhanced ultrasound (45), and SMI may also help prevent ischemic stroke (46). However, measuring ultrasonic parameters close to plaques requires a great deal of clinical expertise and superior image post-processing methods. According to studies, CIMT

Table 4 Comparison of the ability of different models to predict vulnerable plaques

Models	AUC (95% CI)	Cut-off value	Sensitivity (%)	Specificity (%)	△AUC#	P value
GSM	0.669 (0.529–0.790)	30.67	65	75	0.280	<0.001*
SMI level	0.771 (0.629–0.879)	0	86	71	0.174	0.012*
TPA	0.858 (0.738–0.938)	73.67 mm^2	77	92	0.091	0.016*
CIMT	0.673 (0.533–0.793)	0.813 mm	77	54	0.276	<0.001*
CIT	0.849 (0.727–0.932)	0.367 mm	68	92	0.100	0.049*
Combined model	0.949 (0.854–0.990)	0.71	84	96	–	–

△AUC#, values were calculated as changes from the combined model. *, the values are statistically significant. AUC, area under the receiver operating characteristic curve; CI, confidence interval; GSM, greyscale median; SMI, superb microvascular imaging; TPA, total plaque area; CIMT, carotid intima-media thickness; CIT, carotid intima thickness.

and CP progression are closely related to one another (47-49). In individuals with mild carotid stenosis, CIMT was shown to be linked to plaque thickness and TPA and to independently predict incident CP formation (50,51). Our research revealed a strong relationship between CIT and SMI and TPA in advanced plaques. Plaques advance along the carotid in the axis of flow 2.4 times quicker than they thicken, which is a good indicator of the plaque lipid burden, and CIT thickening is also primarily arises from subintimal lipid deposition (43,52). Given these identical pathogenic processes, CIT thickening and TPA elevation occur concurrently but to different degrees during the CP development process. From this, we deduced that in individuals with advanced CP, CIT would be more effectively related to CP than CIMT.

It is generally understood that CIMT is not only a subclinical marker for predicting atherosclerosis (17,50) but is also crucial in stroke diagnosis (51). It commonly accepted that increased CIMT and plaque merely represent quantitatively different phenotypes of a common atherosclerotic background (53), CIMT progression interventions reduce CV risk (54), and CIMT is associated with the incidence of CV events and CV risk factors (55). However, the combination of carotid medium thickness, a factor prone to hypertension, and age, challenges the therapeutic relevance of CIMT.

Recent research by Jin *et al.* showed that radial intima thickness plays a significant role in the differential identification of stroke subtypes (24), indicating the significance of intimal thickness in clinical studies. However, the connection between CIT and the plaque types, which were strongly linked to plaque vulnerability and adverse CV events, was not further explored. In this study, we discovered that higher plaque vulnerability was associated with thicker CIT, larger lipid cores, increased fibrous cap cell infiltration, and increased IPH. Atherosclerosis is an inflammatory process whereby plaque formation begins with pathological intimal thickening and lesions containing lipid pools (56,57). The high correlation between CCA-CIT and lipid core and inflammatory processes in CP also demonstrates the concept of progressive diffuse carotid disease, with significant stenosis at the site of bifurcation having its roots clearly defined at the proximal segment of the artery (58,59).

Previous research has shown the utility of the CIMT, IPN, GSM, and TPA in assessing plaque vulnerability (60-63); however, these studies only examined the value of a single plaque characteristic or CCA, and the role of CIT in assessing plaque vulnerability is still unknown. In this study, we investigated the relative merits of CCA ultrasonic features and plaque ultrasonic features in determining plaque vulnerability. According to our research, among the plaque ultrasonic features, the TPA is a stronger predictor for determining plaque vulnerability than the GSM or SMI. Our study first used CIT to evaluate plaque vulnerability and discovered that CIT was more accurate than CIMT in predicting plaque vulnerability. In terms of histology, the IMT corresponds to the intima-media complex, which comprises endothelial cells, connective tissue, and smooth muscle cells, and represents the site of lipid deposition in plaque development (64). In states of health, ~97.5% of the IMT complex comprises the media, whereas in the presence of atherosclerotic disease, while the intimal contribution to the IMT complex is relatively higher, an estimated 80% of the IMT complex is still formed by the media (47,65). There are several factors that affect media thickness. In a population-based cohort study, Ferreira *et al.* discovered that media thickness is regulated by hypertension (particularly SBP), and is also substantially influenced by age and genetics (66). Therefore, it is more likely that CIT and plaque (rather than CIMT) represent quantitatively different phenotypes of a common atherosclerotic background. Thus, just as CIMT is a good indicator in guiding the use of statins in treating patients with atherosclerosis (67), CIT measurements based on machine learning and artificial intelligence can also be used to facilitate atherosclerosis management. Our study revealed that both TPA and CIT had significant utility in determining plaque vulnerability when we compared the ultrasonic characteristics of plaque and CCA. To diagnose plaque vulnerability, a combined model of CIT representing CCA status and TPA reflecting plaque state was developed. The results revealed that the combined model was able to more comprehensively assess atherosclerotic plaque and had a higher diagnostic value than either factor alone.

Our study had some limitations. First, this study only included 55 patients and was conducted in a single center. Therefore, a study with a larger sample size needs to be conducted to support the study's findings. Second, the pathological analysis in this study used simple semiquantitative scales, which are subjective to some extent and may skew the research outcomes. Finally, no additional grouping was made in the study based on prior drug use (such as statins), and more research is required to examine how medications affect alterations in the correlation between CIT and plaque vulnerability.

Conclusions

In conclusion, we found a relationship between CIT and carotid bifurcation stenosis. Further, we suggest that evaluations that combine CIT and TPA may have a complementary advantage in detecting vulnerable plaque. Hence, the additional measurement of CIT may prove valuable in the identification of vulnerable plaque and patients with advanced CP might benefit from early detection.

Acknowledgments

Funding: This work was supported by the National Key Research and Development Program of China (2022YFC3602403), the grants of the National Natural Science Foundation of China (Nos. 81970377, 82001834) and the Non-profit Central Research Institute Fund of Chinese Academy of Medical Sciences (2023-PT320-06).

Footnote

Reporting Checklist: The authors have completed the STARD reporting checklist. Available at https://qims.amegroups.com/article/view/10.21037/qims-23-1193/rc

Conflicts of Interest: All authors have completed the ICMJE uniform disclosure form (available at https://qims.amegroups.com/article/view/10.21037/qims-23-1193/coif). The authors have no conflicts of interest to declare.

Ethical Statement: The authors are accountable for all aspects of the work in ensuring that questions related to the accuracy or integrity of any part of the work are appropriately investigated and resolved. The study was conducted in accordance with the Declaration of Helsinki (as revised in 2013). The study was approved by the Ethics Committee of Shandong University Qilu Hospital (No. KYLL-2020-183) and informed consent was obtained from all the patients.

References

1. Libby P, Buring JE, Badimon L, Hansson GK, Deanfield J, Bittencourt MS, Tokgözoğlu L, Lewis EF. Atherosclerosis. Nat Rev Dis Primers 2019;5:56.
2. Benjamin EJ, Blaha MJ, Chiuve SE, Cushman M, Das SR, Deo R, et al. Heart Disease and Stroke Statistics-2017 Update: A Report From the American Heart Association. Circulation 2017;135:e146-603.
3. Lusis AJ. Atherosclerosis. Nature 2000;407:233-41.
4. Kobiyama K, Ley K. Atherosclerosis. Circ Res 2018;123:1118-20.
5. Naghavi M, Libby P, Falk E, Casscells SW, Litovsky S, Rumberger J, et al. From vulnerable plaque to vulnerable patient: a call for new definitions and risk assessment strategies: Part I. Circulation 2003;108:1664-72.
6. Holm Nielsen S, Jonasson L, Kalogeropoulos K, Karsdal MA, Reese-Petersen AL, Auf dem Keller U, Genovese F, Nilsson J, Goncalves I. Exploring the role of extracellular matrix proteins to develop biomarkers of plaque vulnerability and outcome. J Intern Med 2020;287:493-513.
7. Semb AG, Rollefstad S, Provan SA, Kvien TK, Stranden E, Olsen IC, Hisdal J. Carotid plaque characteristics and disease activity in rheumatoid arthritis. J Rheumatol 2013;40:359-68.
8. Croca SC, Griffin M, Farinha F, Isenberg DA, Nicolaides A, Rahman A. Total plaque area and plaque echogenicity are novel measures of subclinical atherosclerosis in patients with systemic lupus erythematosus. Rheumatology (Oxford) 2021;60:4185-98.
9. Mathiesen EB, Johnsen SH, Wilsgaard T, Bønaa KH, Løchen ML, Njølstad I. Carotid plaque area and intima-media thickness in prediction of first-ever ischemic stroke: a 10-year follow-up of 6584 men and women: the Tromsø Study. Stroke 2011;42:972-8.
10. Perez HA, Garcia NH, Spence JD, Armando LJ. Adding carotid total plaque area to the Framingham risk score improves cardiovascular risk classification. Arch Med Sci 2016;12:513-20.
11. Inaba Y, Chen JA, Bergmann SR. Carotid plaque, compared with carotid intima-media thickness, more accurately predicts coronary artery disease events: a meta-analysis. Atherosclerosis 2012;220:128-33.
12. Virmani R, Kolodgie FD, Burke AP, Finn AV, Gold HK, Tulenko TN, Wrenn SP, Narula J. Atherosclerotic plaque progression and vulnerability to rupture: angiogenesis as

a source of intraplaque hemorrhage. Arterioscler Thromb Vasc Biol 2005;25:2054-61.
13. Zhang H, Du J, Wang H, Wang H, Jiang J, Zhao J, Lu H. Comparison of diagnostic values of ultrasound microflow imaging and contrast-enhanced ultrasound for neovascularization in carotid plaques. Exp Ther Med 2017;14:680-8.
14. Wang Y, Yao M, Zou M, Li S, Ge Z, Hong Y, Cai S, Wang H, Li J. Assessment of Carotid Intraplaque Neovascularization Using Superb Microvascular Imaging in High Risk of Stroke Individuals: Results From a Community-Based Study. Front Neurol 2019;10:1146.
15. Hoshino M, Shimizu T, Ogura H, Hagiwara Y, Takao N, Soga K, Usuki N, Moriya J, Nakamura H, Hasegawa Y. Intraplaque Microvascular Flow Signal in Superb Microvascular Imaging and Magnetic Resonance Imaging Carotid Plaque Imaging in Patients with Atheromatous Carotid Artery Stenosis. J Stroke Cerebrovasc Dis 2018;27:3529-34.
16. Forsberg F, Machado P, Stanczak M, Farber J, DiMuzio P, Needleman L. Assessing carotid plaque neovascularity and calcifications in patients prior to endarterectomy. J Vasc Surg 2019;70:1137-44.
17. O'Leary DH, Polak JF, Kronmal RA, Manolio TA, Burke GL, Wolfson SK Jr. Carotid-artery intima and media thickness as a risk factor for myocardial infarction and stroke in older adults. Cardiovascular Health Study Collaborative Research Group. N Engl J Med 1999;340:14-22.
18. Nikic P, Savic M, Jakovljevic V, Djuric D. Carotid atherosclerosis, coronary atherosclerosis and carotid intima-media thickness in patients with ischemic cerebral disease: Is there any link? Exp Clin Cardiol 2006;11:102-6.
19. Brunelli N, Altamura C, Costa CM, Altavilla R, Palazzo P, Maggio P, Marcosano M, Vernieri F. Carotid Artery Plaque Progression: Proposal of a New Predictive Score and Role of Carotid Intima-Media Thickness. Int J Environ Res Public Health 2022;19:758.
20. Rundek T, Gardener H, Della-Morte D, Dong C, Cabral D, Tiozzo E, Roberts E, Crisby M, Cheung K, Demmer R, Elkind MS, Sacco RL, Desvarieux M. The relationship between carotid intima-media thickness and carotid plaque in the Northern Manhattan Study. Atherosclerosis 2015;241:364-70.
21. Tschiderer L, Klingenschmid G, Seekircher L, Willeit P. Carotid intima-media thickness predicts carotid plaque development: Meta-analysis of seven studies involving 9341 participants. Eur J Clin Invest 2020;50:e13217.
22. Insull W Jr. The pathology of atherosclerosis: plaque development and plaque responses to medical treatment. Am J Med 2009;122:S3-S14.
23. Xu M, Zhang M, Xu J, Zhu M, Zhang C, Zhang P, Zhang Y. The independent and add-on values of radial intima thickness measured by ultrasound biomicroscopy for diagnosis of coronary artery disease. Eur Heart J Cardiovasc Imaging 2019;20:889-96.
24. Jin S, Zhang C, Zhang Y, Jia G, Zhang M, Xu M. Differential value of intima thickness in ischaemic stroke due to large-artery atherosclerosis and small-vessel occlusion. J Cell Mol Med 2021;25:9427-33.
25. Bakris G, Ali W, Parati G. ACC/AHA Versus ESC/ESH on Hypertension Guidelines: JACC Guideline Comparison. J Am Coll Cardiol 2019;73:3018-26.
26. Diagnosis and classification of diabetes mellitus. Diabetes Care 2010;33 Suppl 1:S62-9.
27. Casella IB, Fukushima RB, Marques AB, Cury MV, Presti C. Comparison between a new computer program and the reference software for gray-scale median analysis of atherosclerotic carotid plaques. J Clin Ultrasound 2015;43:194-8.
28. Sabetai MM, Tegos TJ, Nicolaides AN, Dhanjil S, Pare GJ, Stevens JM. Reproducibility of computer-quantified carotid plaque echogenicity: can we overcome the subjectivity? Stroke 2000;31:2189-96.
29. Zamani M, Skagen K, Scott H, Lindberg B, Russell D, Skjelland M. Carotid Plaque Neovascularization Detected With Superb Microvascular Imaging Ultrasound Without Using Contrast Media. Stroke 2019;50:3121-7.
30. Carvalho-Romano LFRS, Bonafé RP, Paim LR, Marques ER, Vegian CFL, Pio-Magalhães JA, Mello DSS, de Rossi G, Coelho-Filho OR, Schreiber R, Sposito AC, Matos-Souza JR, Nadruz W Jr. Association of carotid wall layers with atherosclerotic plaques and cardiac hypertrophy in hypertensive subjects. J Hum Hypertens 2022;36:732-7.
31. Martins NS, Barreto J, Kimura-Medorima ST, Vitte SH, Quinaglia T, Assato B, Coelho-Filho OR, Matos-Souza JR, Nadruz W, Sposito AC; Brazilian Heart Study Group. Carotid intima layer thickness but not intima-media thickness is related to coronary artery calcification in type 2 diabetes individuals: Results from the Brazilian diabetes study. Nutr Metab Cardiovasc Dis 2023;33:2384-8.
32. Lovett JK, Gallagher PJ, Hands LJ, Walton J, Rothwell PM. Histological correlates of carotid plaque surface morphology on lumen contrast imaging. Circulation 2004;110:2190-7.
33. Obaid DR, Calvert PA, Gopalan D, Parker RA, Hoole

SP, West NE, Goddard M, Rudd JH, Bennett MR. Atherosclerotic plaque composition and classification identified by coronary computed tomography: assessment of computed tomography-generated plaque maps compared with virtual histology intravascular ultrasound and histology. Circ Cardiovasc Imaging 2013;6:655-64.
34. Mushenkova NV, Summerhill VI, Zhang D, Romanenko EB, Grechko AV, Orekhov AN. Current Advances in the Diagnostic Imaging of Atherosclerosis: Insights into the Pathophysiology of Vulnerable Plaque. Int J Mol Sci 2020;21:2992.
35. Ichikawa K, Miyoshi T, Osawa K, Miki T, Ito H. Increased Circulating Malondialdehyde-Modified Low-Density Lipoprotein Level Is Associated with High-Risk Plaque in Coronary Computed Tomography Angiography in Patients Receiving Statin Therapy. J Clin Med 2021;10:1480.
36. Weng ST, Lai QL, Cai MT, Wang JJ, Zhuang LY, Cheng L, Mo YJ, Liu L, Zhang YX, Qiao S. Detecting vulnerable carotid plaque and its component characteristics: Progress in related imaging techniques. Front Neurol 2022;13:982147.
37. Du H, Yang W, Chen X. Histology-Verified Intracranial Artery Calcification and Its Clinical Relevance With Cerebrovascular Disease. Front Neurol 2021;12:789035.
38. Corti R, Fuster V, Badimon JJ, Hutter R, Fayad ZA. New understanding of atherosclerosis (clinically and experimentally) with evolving MRI technology in vivo. Ann N Y Acad Sci 2001;947:181-95; discussion 195-8.
39. Jiang C, Meng Q, Zhao K, Zhao H, Zheng Z, Wu W, Zhao X. Vulnerable carotid plaque characteristics on magnetic resonance vessel wall imaging: potential predictors for hemodynamic instability during carotid artery stenting. Quant Imaging Med Surg 2023;13:3441-50.
40. Gonçalves I, den Ruijter H, Nahrendorf M, Pasterkamp G. Detecting the vulnerable plaque in patients. J Intern Med 2015;278:520-30.
41. Hellings WE, Peeters W, Moll FL, Piers SR, van Setten J, Van der Spek PJ, de Vries JP, Seldenrijk KA, De Bruin PC, Vink A, Velema E, de Kleijn DP, Pasterkamp G. Composition of carotid atherosclerotic plaque is associated with cardiovascular outcome: a prognostic study. Circulation 2010;121:1941-50.
42. El-Barghouty NM, Levine T, Ladva S, Flanagan A, Nicolaides A. Histological verification of computerised carotid plaque characterisation. Eur J Vasc Endovasc Surg 1996;11:414-6.
43. Azarpazhooh MR, Mathiesen E, Rundek T, Romanens M, Adams A, Armando L, Perez H, Villafañe H, Garcia NH, Ibañez B, Bogiatzi C, Tabrizi R, Fuster V, Spence JD. Reliability, Reproducibility, and Advantages of Measuring Carotid Total Plaque Area. J Am Soc Echocardiogr 2022;35:530-2.
44. Barnett PA, Spence JD, Manuck SB, Jennings JR. Psychological stress and the progression of carotid artery disease. J Hypertens 1997;15:49-55.
45. Oura K, Kato T, Ohba H, Terayama Y. Evaluation of Intraplaque Neovascularization Using Superb Microvascular Imaging and Contrast-Enhanced Ultrasonography. J Stroke Cerebrovasc Dis 2018;27:2348-53.
46. Yang DB, Zhou J, Feng L, Xu R, Wang YC. Value of superb micro-vascular imaging in predicting ischemic stroke in patients with carotid atherosclerotic plaques. World J Clin Cases 2019;7:839-48.
47. Yang Y, Fan F, Gao L, Han X, Cheng G, Jia J, Zhang B, Ma W, Huo Y, Qi L, Zhang Y. The relationship between carotid intima-media thickness and carotid plaque: a cohort study in China. J Hum Hypertens 2020;34:468-73.
48. Centurión OA. Carotid Intima-Media Thickness as a Cardiovascular Risk Factor and Imaging Pathway of Atherosclerosis. Crit Pathw Cardiol 2016;15:152-60.
49. von Sarnowski B, Lüdemann J, Völzke H, Dörr M, Kessler C, Schminke U. Common carotid intima-media thickness and framingham risk score predict incident carotid atherosclerotic plaque formation: longitudinal results from the study of health in Pomerania. Stroke 2010;41:2375-7.
50. O'Leary DH, Polak JF, Kronmal RA, Savage PJ, Borhani NO, Kittner SJ, Tracy R, Gardin JM, Price TR, Furberg CD. Thickening of the carotid wall. A marker for atherosclerosis in the elderly? Cardiovascular Health Study Collaborative Research Group. Stroke 1996;27:224-31.
51. Tsivgoulis G, Vemmos KN, Spengos K, Papamichael CM, Cimboneriu A, Zis V, Zakopoulos N, Mavrikakis M. Common carotid artery intima-media thickness for the risk assessment of lacunar infarction versus intracerebral haemorrhage. J Neurol 2005;252:1093-100.
52. Al-Shali K, House AA, Hanley AJ, Khan HM, Harris SB, Mamakeesick M, Zinman B, Fenster A, Spence JD, Hegele RA. Differences between carotid wall morphological phenotypes measured by ultrasound in one, two and three dimensions. Atherosclerosis 2005;178:319-25.
53. Di Bello V, Carerj S, Perticone F, Benedetto F, Palombo C, Talini E, Giannini D, La Carrubba S, Antonini-Canterin F, Di Salvo G, Bellieni G, Pezzano A, Romano MF, Balbarini A; Research Group of the Italian Society of CardioVascular Echocardiography (SIEC). Carotid intima-media thickness

in asymptomatic patients with arterial hypertension without clinical cardiovascular disease: relation with left ventricular geometry and mass and coexisting risk factors. Angiology 2009;60:705-13.
54. Willeit P, Tschiderer L, Allara E, Reuber K, Seekircher L, Gao L, et al. Carotid Intima-Media Thickness Progression as Surrogate Marker for Cardiovascular Risk: Meta-Analysis of 119 Clinical Trials Involving 100 667 Patients. Circulation 2020;142:621-42.
55. Kabłak-Ziembicka A, Przewłocki T. Clinical Significance of Carotid Intima-Media Complex and Carotid Plaque Assessment by Ultrasound for the Prediction of Adverse Cardiovascular Events in Primary and Secondary Care Patients. J Clin Med 2021;10:4628.
56. Finn AV, Kolodgie FD, Virmani R. Correlation between carotid intimal/medial thickness and atherosclerosis: a point of view from pathology. Arterioscler Thromb Vasc Biol 2010;30:177-81.
57. Steinbuch J, van Dijk AC, Schreuder F, Truijman M, Hendrikse J, Nederkoorn PJ, van der Lugt A, Hermeling E, Hoeks A, Mess WH. Definition of common carotid wall thickness affects risk classification in relation to degree of internal carotid artery stenosis: the Plaque At RISK (PARISK) study. Cardiovasc Ultrasound 2017;15:9.
58. Ibrahimi P, Jashari F, Johansson E, Grönlund C, Bajraktari G, Wester P, Henein MY. Common carotid intima-media features determine distal disease phenotype and vulnerability in asymptomatic patients. Int J Cardiol 2015;196:22-8.
59. Golinvaux N, Maehara A, Mintz GS, Lansky AJ, McPherson J, Farhat N, Marso S, de Bruyne B, Serruys PW, Templin B, Cheong WF, Aaskar R, Fahy M, Mehran R, Leon M, Stone GW. An intravascular ultrasound appraisal of atherosclerotic plaque distribution in diseased coronary arteries. Am Heart J 2012;163:624-31.
60. Grobbee DE, Bots ML. Atherosclerotic disease regression with statins: studies using vascular markers. Int J Cardiol 2004;96:447-59.
61. van Hinsbergh VW, Eringa EC, Daemen MJ. Neovascularization of the atherosclerotic plaque: interplay between atherosclerotic lesion, adventitia-derived microvessels and perivascular fat. Curr Opin Lipidol 2015;26:405-11.
62. Salem MK, Bown MJ, Sayers RD, West K, Moore D, Nicolaides A, Robinson TG, Naylor AR. Identification of patients with a histologically unstable carotid plaque using ultrasonic plaque image analysis. Eur J Vasc Endovasc Surg 2014;48:118-25.
63. Mitchell CC, Stein JH, Cook TD, Salamat S, Wang X, Varghese T, Jackson DC, Sandoval Garcia C, Wilbrand SM, Dempsey RJ. Histopathologic Validation of Grayscale Carotid Plaque Characteristics Related to Plaque Vulnerability. Ultrasound Med Biol 2017;43:129-37.
64. Stary HC, Chandler AB, Glagov S, Guyton JR, Insull W Jr, Rosenfeld ME, Schaffer SA, Schwartz CJ, Wagner WD, Wissler RW. A definition of initial, fatty streak, and intermediate lesions of atherosclerosis. A report from the Committee on Vascular Lesions of the Council on Arteriosclerosis, American Heart Association. Circulation 1994;89:2462-78.
65. Spence JD. Ultrasound measurement of carotid plaque as a surrogate outcome for coronary artery disease. Am J Cardiol 2002;89:10B-15B; discussion 15B-16B.
66. Ferreira JP, Girerd N, Bozec E, Machu JL, Boivin JM, London GM, Zannad F, Rossignol P. Intima-Media Thickness Is Linearly and Continuously Associated With Systolic Blood Pressure in a Population-Based Cohort (STANISLAS Cohort Study). J Am Heart Assoc 2016;5:e003529.
67. Formanowicz D, Krawczyk JB, Perek B, Lipski D, Tykarski A. Management of High-Risk Atherosclerotic Patients by Statins May Be Supported by Logistic Model of Intima-Media Thickening. J Clin Med 2021;10:2876.

Cite this article as: Zhao YC, Zhang J, Wang F, He YM, Xu MJ, Wang DH, Zhang M. Value of carotid intima thickness in assessing advanced carotid plaque vulnerability: a study based on carotid artery ultrasonography and carotid plaque histology. Quant Imaging Med Surg 2024;14(2):1994-2007. doi: 10.21037/qims-23-1193

